

THE ELECTROSTATIC POTENTIAL ASSOCIATED TO INTERFACE PHONON MODES IN NITRIDE SINGLE HETEROSTRUCTURES

M. E. Mora-Ramos and R. Pérez-Alvarez

Facultad de Ciencias
Universidad Autónoma del Estado de Morelos
Mexico

V. R. Velasco

Instituto de Ciencia de Materiales de Madrid
CSIC
Spain

Abstract—The electrostatic potential associated to the interface oscillation modes in nitride-based heterostructure is calculated with the use of a complete phenomenological electroelastic continuum approach for the long wave optical oscillations, and the Surface Green Function Matching technique. The crystalline symmetries of zincblende and — isotropically averaged — wurtzite are both considered in the sets of input bulk frequencies and dielectric constants.

1. INTRODUCTION

The description of the long wavelength polar optical modes in nitride-based heterostructures with wurtzite structure has been put forward since the mid nineties within a formalism that combines the so-called dielectric continuum model (DCM) together with the Loudon's uniaxial model [1]. Studies on the subject have continued until very recently [2–4]. In these works, different polar optical phonon branches have been identified as interface modes, half-space modes, confined or quasi-confined modes, and propagating modes. At the same time, the corresponding electron-phonon interaction Hamiltonians were derived.

In a recent paper Mora-Ramos et al. [5] calculated the interface-polar-optical-phonon-limited mobility for electrons in the conduction band of AlGa_N/Ga_N single heterostructures using the model and

interaction Hamiltonian presented in [1]. The outcome of their calculation revealed values for the room temperature mobility well below the most of the experimental reports in such kind of systems. Since several different approaches for the calculation of single electron conduction band states were tested, the problem seems to be related with the particular approach for the optical phonon modes that arises from the uniaxial DCM.

The discussion about the suitability of the DCM for a complete phenomenological description of the optical phonon in polar semiconducting heterostructures dates back to the early nineties [6, 7]. The limitation of the DCM for dealing with the mechanical boundary conditions was then highlighted, and a continuum phenomenological electroelastic model (CPELM) was proposed instead. This model was later applied to the study of polar optical phonon modes in AlGaAs/GaAs single heterostructures [8], in combination with the method of Surface Green Function Matching (SGFM).

2. SOME COMMENTS ON THE THEORY

We will use the CPELM-SGFM formalism in the present article. Due to its rather involved mathematical framework, the reader is referred to references [6–9] for details.

The CPELM deals exclusively with systems made of semiconductors with cubic crystalline symmetry. Nevertheless, we believe that some new information, regarding the interface phonon modes, can be derived with its application to heterostructures of materials bearing hexagonal symmetry such as the wurtzite nitrides. For this purpose, the procedure implies the isotropic averaging of the main input parameters of the model. These are the bulk longitudinal and transversal phonon frequencies at the Brillouin Zone center, and the dielectric constants. Besides, it is also needed to average the values of the parameters β_L , and β_T . They are related to the phonon dispersion curves in the bulk, which can be well approximated by $\omega_L^2(q) = \omega_{LO}^2 - \beta_L^2 q^2$, and by $\omega_T^2(q) = \omega_{TO}^2 - \beta_T^2 q^2$, for the longitudinal and transversal phonons respectively. Since the CPELM is a long wavelength model, its application is usually restricted to a small region — of about 10% — of the Brillouin zone, around the Γ point. This is precisely the region where the parabolic approximation of the dispersion relation appropriately applies.

The work is restricted to deal with GaN-AlGaN structures. We are considering a system that consists of two half-space layers. The one made of $\text{Al}_x\text{Ga}_{1-x}\text{N}$ is located at the $z < 0$ region, while for $z > 0$ we have the GaN. For the case of zincblende materials we use

the following input parameters: $\epsilon_\infty(GaN) = 5.30$, $\epsilon_\infty(AlN) = 4.46$; $\rho(GaN) = 6.10 \text{ g/cm}^3$, $\rho(AlN) = 3.29 \text{ g/cm}^3$; $\omega_{LO}(GaN) = 748 \text{ cm}^{-1}$, $\omega_{LO}(AlN) = 920 \text{ cm}^{-1}$; $\omega_{TO}(GaN) = 562 \text{ cm}^{-1}$, $\omega_{TO}(AlN) = 670 \text{ cm}^{-1}$; $\beta_L^2(GaN) = 1.52 \times 10^{-11}$, $\beta_L^2(AlN) = 1.44 \times 10^{-11}$; $\beta_T^2(GaN) = 2.87 \times 10^{-13}$, $\beta_T^2(AlN) = 5.89 \times 10^{-12}$. The corresponding expressions for the cubic alloy $Al_xGa_{1-x}N$ are obtained by applying the Vegard's law to each of them. That is, $f(Al_xGa_{1-x}N) = f(GaN) * (1 - x) + f(AlN) * x$.

In the case of the wurtzite nitrides, we have: $\epsilon_\infty(GaN) = 5.29$, $\epsilon_\infty(AlN) = 4.68$; $\rho(GaN) = 6.15 \text{ g/cm}^3$, $\rho(AlN) = 3.23 \text{ g/cm}^3$, with their corresponding Vegard's laws. On the other hand, the parabolic dispersion amplitudes are: $\beta_{zL}^2(GaN) = 2.78 \times 10^{-12}$, $\beta_{zL}^2(AlN) = 2.47 \times 10^{-11}$; $\beta_{\perp L}^2(GaN) = 7.60 \times 10^{-12}$, $\beta_{\perp L}^2(AlN) = 2.28 \times 10^{-11}$; $\beta_{zT}^2(GaN) = -2.53 \times 10^{-12}$, $\beta_{zT}^2(AlN) = 7.34 \times 10^{-12}$; $\beta_{\perp T}^2(GaN) = -1.21 \times 10^{-12}$, $\beta_{\perp T}^2(AlN) = 2.69 \times 10^{-12}$; Vegard's law is also applied to these quantities, in order to deal with their values for the alloy.

The indexes "z" and " \perp " label the $A1$ and $E1$ infrared-active polar optical mode of the wurzite structure, respectively. The dependencies of the frequencies of these optical modes upon the aluminum molar fraction have been studied in greater detail. The longitudinal modes have a one-mode character. The corresponding frequencies are: $\omega_{zL} = 734 + 153x + 75x(1 - x) \text{ cm}^{-1}$, $\omega_{\perp L} = 7442 + 170x + 65x(1 - x) \text{ cm}^{-1}$. The transversal modes have two-mode character, GaN-like and AlN-like, with frequencies given by: $\omega_z(GaN) = 532 + 65x - 2x(1 - x) \text{ cm}^{-1}$, $\omega_z(AlN) = 551 + 55x$; $\omega_{\perp}(GaN) = 557 + 53x \text{ cm}^{-1}$, $\omega_{\perp}(AlN) = 617 + 47x \text{ cm}^{-1}$. All these data have been collected from different works (see references [10–16]). To grant the application of the CPELM to the wurtzite heterostructures, the "z" and " \perp " values are isotropically averaged.

3. RESULTS AND CONCLUSIONS

Figures 1 and 2 show the local density of states (LDOS) for SHS with cubic and hexagonal symmetry, respectively. The peaks correspond to the value of the interface polar optical phonon oscillations. The set of LDOS peaks for different values of the phonon wavevector κ generates the dispersion relation of the interface mode. These dispersion relations for nitride SHS are shown in Figure 3 for some values of the Al molar fraction x .

Figures 4 and 5 present the electrostatic potential corresponding to the GaN-like interface mode in wurtzite and zincblende $Al_xGa_{1-x}N/GaN$ SHS respectively. The values of the phonon wavevector in each case have been chosen just for illustration. A slight oscilla-

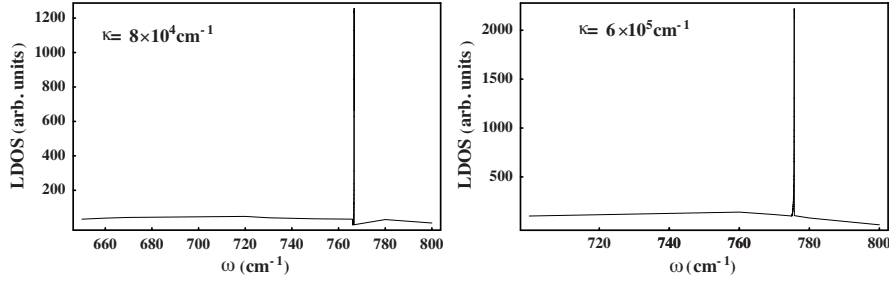


Figure 1. LDOS in a zincblende $\text{Al}_{0.22}\text{Ga}_{0.78}\text{N}/\text{GaN}$ SHS for phonon wavevector $\kappa = 8 \times 10^4 \text{ cm}^{-1}$ SHS (left), and for a zincblende $\text{Al}_{0.33}\text{Ga}_{0.67}\text{N}/\text{GaN}$ SHS for wavevector $\kappa = 6 \times 10^5 \text{ cm}^{-1}$ SHS (right).

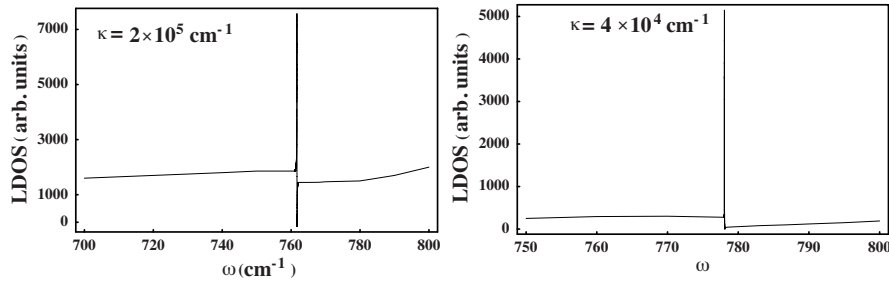


Figure 2. LDOS in a wurtzite $\text{Al}_{0.22}\text{Ga}_{0.78}\text{N}/\text{GaN}$ SHS for phonon wavevector $\kappa = 2 \times 10^5 \text{ cm}^{-1}$ SHS (left), and for a wurtzite $\text{Al}_{0.40}\text{Ga}_{0.60}\text{N}/\text{GaN}$ SHS for wavevector $\kappa = 4 \times 10^4 \text{ cm}^{-1}$ SHS (right).

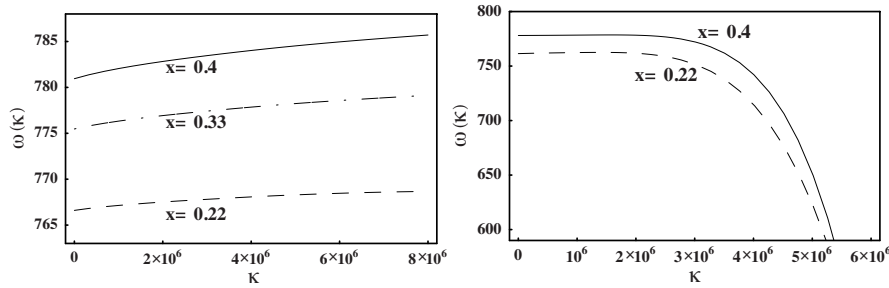


Figure 3. Dispersion relations for the interface polar optical oscillation mode in zincblende $\text{Al}_x\text{Ga}_{1-x}\text{N}/\text{GaN}$ SHS (left), and wurtzite $\text{Al}_x\text{Ga}_{1-x}\text{N}/\text{GaN}$ SHS (right).

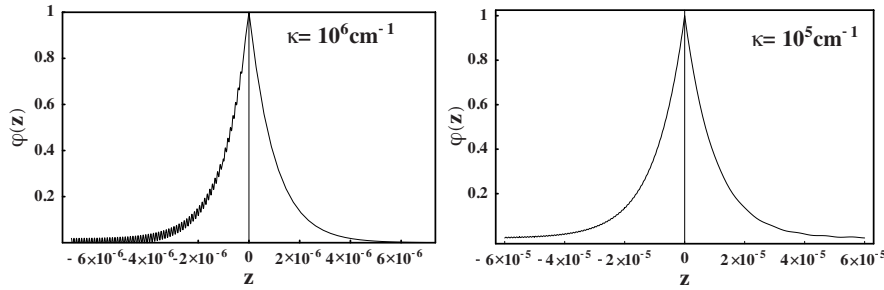


Figure 4. Electrostatic potential function corresponding to the GaN-like interface phonon mode in wurtzite $\text{Al}_x\text{Ga}_{1-x}\text{N}/\text{GaN}$ SHS. In this case: $x = 0.22$, $\kappa = 10^6 \text{ cm}^{-1}$ (left), and $x = 0.33$, $\kappa = 10^5 \text{ cm}^{-1}$ (right). Arbitrary units are used on both axes.

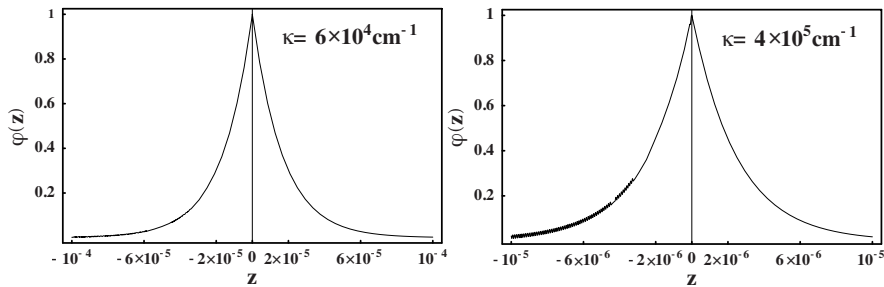


Figure 5. Electrostatic potential function corresponding to the GaN-like interface phonon mode in zincblende $\text{Al}_x\text{Ga}_{1-x}\text{N}/\text{GaN}$ SHS. In this case: $x = 0.33$, $\kappa = 6 \times 10^4 \text{ cm}^{-1}$ (left), and $x = 0.40$, $\kappa = 4 \times 10^5 \text{ cm}^{-1}$ (right). Arbitrary units are used on both axes.

tory behavior is observed on the AlGa_N side of the SHS. In fact, the amplitude of the small oscillations of ϕ in that region depends on the magnitude of the phonon wavevector. It is more apparent for higher values of κ . To explain this, one should remember that we are studying the GaN-like modes only. For these modes it fulfills that $\omega(\kappa) < \omega_{LO}$ in the region $z < 0$.

The decaying behavior of φ is readily noticed. It is, in fact, very stepped. Consequently, the width of the region of penetration is extremely narrow. This suggests that the actual contribution of this mode to the electron-phonon matrix elements might be significantly low. Work on this subject is in progress.

ACKNOWLEDGMENT

M. E. M. R. acknowledges support from CONACyT through Grant 52304.

REFERENCES

1. Lee, B. C., K. W. Kim, M. A. Stroscio, and M. Dutta, "Optical-phonon confinement and scattering in wurtzite heterostructures," *Phys. Rev. B*, Vol. 58, No. 8, 4860–4865, 1998.
2. Shi, J.-J., "Interface optical phonon modes and electron-interface-phonon interactions in wurtzite GaN/AlN quantum wells," *Phys. Rev. B*, Vol. 68, No. 16, 165335(1)–165335(11), 2003.
3. Shi, J.-J., X. L. Chu, and E. M. Goldys, "Propagating optical-phonon modes and their electron-phonon interactions in wurtzite GaN/Al_xGa_{1-x}N quantum wells," *Phys. Rev. B*, Vol. 70, No. 11, 115318(1)–115318(8), 2004.
4. Li, L., D. Liu, and J. J. Shi, "Electron-quasi-confined-optical-phonon interactions in wurtzite GaN/AlN quantum wells," *Eur. Phys. J. B*, Vol. 44, No. 4, 401–413, 2005.
5. Mora-Ramos, M. E., J. Tutor, and V. R. Velasco, "Interface-phonon-limited two-dimensional mobility in AlGa_xN/GaN heterostructures," *J. Appl. Phys.*, Vol. 100, No. 12, 123708(1)–123708(9), 2006.
6. Trallero-Giner, C., F. García-Moliner, V. R. Velasco, and M. Cardona, "Analysis of the phenomenological models for long wavelength polar optical modes in semiconductor layered systems," *Phys. Rev. B*, Vol. 45, No. 20, 11944–11948, 1992.
7. García-Moliner, F., "Long wave polar optical phonons in heterostructures," *Phonons in Semiconductor Nanostructures: Proceedings of the NATO Advanced Research Workshop*, J.-P. Leburton, J. Pascual, and C. Sotomayor-Torres (eds.), Kluwer Academic Publishers 1993, 1–12, St. Feliu De Guixols, Spain, September 1992.
8. Chubykalo, A., V. R. Velasco, and F. García-Moliner, "Polar optical phonons at semiconductor interfaces," *Surf. Sci.*, Vol. 319, Nos. 1–2, 184–192, 1994.
9. Mora-Ramos, M. E. and D. A. Contreras-Solorio, "The polaron in a GaAs/AlAs quantum well," *Physica B*, Vol. 253, No. 3-4, 325–334, 1998.
10. Davydov, V. Y., Y. E. Kitaev, I. N. Goncharuk, A. N. Smirnov, J. Graul, O. Semchinova, D. Uffmann, M. B. Smirnov,

- A. P. Mirgorodsky, and R. A. Evarestov, "Phonon dispersion and Raman scattering in hexagonal GaN and AlN," *Phys. Rev. B*, Vol. 58, No. 19, 12899–12907, 1998.
11. Zi, J., X. Wan, G. Wei, K. Zhang, and X. Xie, "Lattice dynamics of zinc-blende GaN and AlN: I. Bulk phonons," *J. Phys.: Cond. Matt.*, Vol. 8, 6323–6328, 1996.
 12. Bechstedt, F. and H. Grille, "Lattice dynamics of ternary alloys," *Phys. Stat. Sol. (B)*, Vol. 216, 761–768, 1999.
 13. Bechstedt, F., J. Furthmüller, and J.-M. Wagner, "Electronic and vibrational properties of group-III nitrides: Ab initio studies," *Phys. Stat. Sol. (C)*, Vol. 0, 1732–1749, 2003.
 14. Santos, A. M., E. C. F. Silva, O. C. Noriega, H. W. L. Alves, J. L. A. Alves, and J. R. Leite, "Vibrational properties of cubic $\text{Al}_x\text{Ga}_{1-x}\text{N}$ and $\text{In}_x\text{Ga}_{1-x}\text{N}$ ternary alloys," *Phys. Stat. Sol. (B)*, Vol. 232, 182–187, 2002.
 15. Bougrov, V., M. E. Levinshtein, S. L. Rumyantsev, and A. Zubrikov, "GaN, AlN, InN, BN, SiC, SiGe," *Properties of Advanced Semiconductor Materials*, M. E. Levinshtein, S. L. Rumyantsev, and M. S. Shur (eds.), John Wiley, New York, 2001.
 16. Palmer, D. W., <http://www.semiconductors.co.uk>.